

Magnetic properties of vanadium-oxide nanotubes probed by static magnetization and ^{51}V NMR

E. Vavilova^{1,2}, I. Hellmann¹, V. Kataev^{1,2}, C. Täschner¹, B. Büchner¹, and R. Klingeler¹

¹*Leibniz-Institute for Solid State and Materials Research IFW Dresden,*

P.O. Box 270116, D-01171 Dresden, Germany and

²*Kazan Physical Technical Institute of the Russian Academy of Sciences, 420029 Kazan, Russia*

(Dated: 29th June 2018)

Measurements of the static magnetic susceptibility and of the nuclear magnetic resonance of multiwalled vanadium-oxide nanotubes are reported. In this nanoscale magnet the structural low-dimensionality and mixed valency of vanadium ions yield a complex temperature dependence of the static magnetization and the nuclear relaxation rates. Analysis of the different contributions to the magnetism allows to identify individual interlayer magnetic sites as well as strongly antiferromagnetically coupled vanadium spins ($S = 1/2$) in the double layers of the nanotube's wall. In particular, the data give strong indications that in the structurally well-defined vanadium-spin chains in the walls, owing to an inhomogeneous charge distribution, antiferromagnetic dimers and trimers occur. Altogether, about 30% of the vanadium ions are coupled in dimers, exhibiting a spin gap of the order of 700 K, the other $\sim 30\%$ comprise individual spins and trimers, whereas the remaining $\sim 40\%$ are nonmagnetic.

PACS numbers: 75.75.+a, 75.40.Cx, 76.60.-k

I. INTRODUCTION

Nanoscale magnetic materials are the subject of a currently increasing interest which is related both to the novel fundamental aspects of magnetic structure and dynamics on the nanometer-scale, and promising future technological applications, such as magnetic data storage elements, sensors or spin electronic devices (for a review see, e.g., Ref. 1). One novel approach to engineer single, i.e. well separated and individually addressable nanoscale magnets, is to utilize self-organization of nanostructures, such as carbon fullerenes, carbon nanotubes, silicon-carbon-nanorods and others. However, owing to a weak magnetic exchange between unpaired spins these materials often exhibit only a very small magnetic moment so that external magnetic fields barely interact with these nanostructures. One possible way to overcome this problem is to prepare self-organized nanoscale materials based on transition-metal (TM) oxide low-dimensional (low-D) structural units where complex strong electronic correlations in the spin- and charge sectors are expected. Indeed, a variety of fascinating phenomena related to spin- and charge correlations in low-D TM oxides were found in the past years, ranging from high-temperature superconductivity in 2D-cuprates, a spin-Peierls transition or a Haldane spin-gap behavior in 1D-spin chain compounds, to superconductivity in 1D-spin ladder materials (for recent reviews see e.g. Ref. 2,3,4,5).

Recently a new class of nanoscale spin magnets, mixed valence vanadium oxide multiwall nanotubes ($\text{VO}_x\text{-NTs}$), has been introduced.⁶ The structure of the $\text{VO}_x\text{-NT}$ walls⁷ is closely related to that of barium vanadium oxide bronze $\text{BaV}_7\text{O}_{16} \times n\text{H}_2\text{O}$ (Fig. 1).⁸ One finds there a V-metal ion in distorted octahedral and tetrahedral coordination, respectively. V-octahedra are coupled in edge-

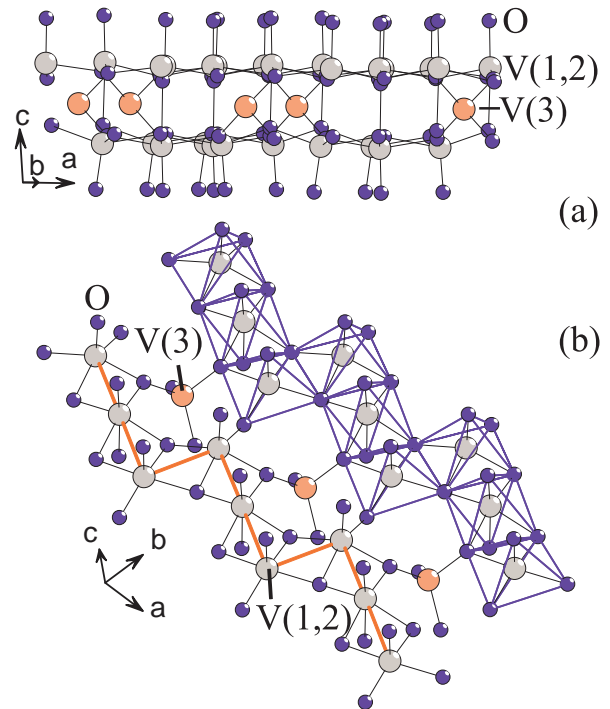


Figure 1: (Color online) Structure of the $\text{VO}_x\text{-NT}$ wall: (a) Double layer of octahedrally coordinated V(1,2) ions. Tetrahedrally coordinated V(3) ions are located between the two layers. (b) Zig-zag V(1,2)-chains in a layer.

sharing zig-zag VO-chains. Arrays of VO-chains form a double layer with tetrahedral V-sites lying between the two layers. Mixed valence vanadium oxides, VO_x ($1.0 < x < 2.5$), are themselves very rich in electronic and magnetic properties owing to an intimate interplay between spin, orbital and charge degrees of freedom.²

When assembled in nanotubes (NT) using dodecylamine, $C_{12}H_{25}NH_2$, as a structure-directing surfactant molecule, VO_x -NTs show up diverse properties ranging from spin frustration and semiconductivity to ferromagnetism by doping with either electrons or holes.⁹ Such a rich behavior makes this material very interesting from the viewpoint of fundamental research as well as regarding possible future applications mentioned above. In particular, its magnetic properties can be widely tuned by intercalation or electrochemical doping (e.g. by lithium or iodine), thereby offering the possibility to realize novel nanoscale magneto-electronic devices. A detailed analysis of the magnetic properties is, therefore, important in order to correlate them with structure and morphology of VO_x -NTs for tailoring the magnetic properties of this nanostructured material.

In order to obtain a deeper insight into the magnetism of VO_x -NTs we have measured magnetization and nuclear magnetic resonance (NMR) of pristine, i.e. Li-undoped, samples. The static magnetic data give evidence for the occurrence of magnetically nonequivalent vanadium sites in the structure. These sites can be presumably attributed to V^{4+} (d^1 , $S = 1/2$) ions in the octahedral and tetrahedral oxygen coordination, respectively. The spins in the octahedral sites (chain sites), are strongly antiferromagnetically correlated. One part of them is coupled in dimers and exhibits a spin-gap behavior. The other part forms trimers. They, together with much weaker correlated tetrahedral magnetic sites, dominate the low-temperature static magnetic response. NMR measurements on ^{51}V nuclei reveal relaxation channels with two distinctly different relaxation rates. Though the longitudinal relaxation rate T_1^{-1} exhibits a strong temperature dependence the manifestation of a spin gap is obscured due to the presence of an appreciable amount of magnetic sites at low temperatures. We discuss possible mechanisms of vanadium nuclear spin relaxation and their interplay with the static magnetic properties. In particular, both NMR and the static susceptibility data give strong indications that owing to the pronounced structural low-dimensionality and mixed valency of VO_x -NTs different spin arrangements, namely individual spins, spin dimers and trimers, coexist in comparable amounts in this complex material.

II. EXPERIMENTAL RESULTS AND DISCUSSION

A. Samples and Experimental

Samples of VO_x -NTs were synthesized using a hydrothermal procedure described in Ref. 6,9. The high quality of the samples has been verified by a number of techniques, such as high-resolution and analytical transmission electron microscopy (TEM), electron diffraction, x-ray photoemission spectroscopy and electron energy-loss spectroscopy (EELS)(for details see Ref. 10). In this

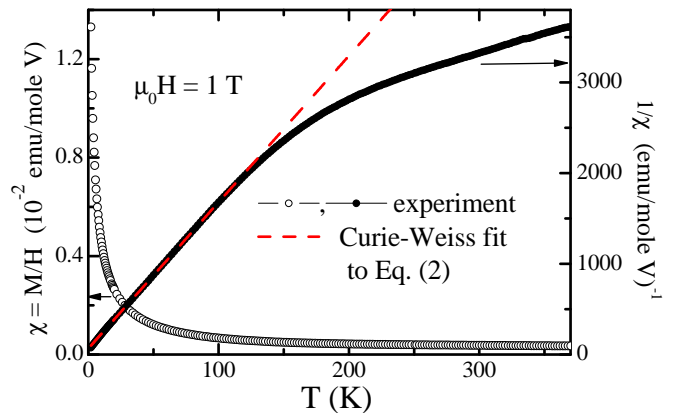


Figure 2: (Color online) Temperature dependence of the static susceptibility $\chi(T) = M(T)/H$ in an external magnetic field of $\mu_0H = 1$ T (left ordinate) and of $1/\chi(T)$ (right ordinate). The dashed line is a Curie-Weiss fit of the low temperature data to Eq. (2). (For details see the text.)

preparation method the nanotubes occur in two topological modifications, i.e. concentric shell tubes with closed edges of the VO_x sheets and scrolled tubes with open edges, with the latter topology being a predominant one.⁶ As one can see in Fig. 1 of Ref. 10, however, the tube walls in our samples consist of a large number (~ 20) of VO_x layers. Therefore one expects that such differences in the microscopic topology, yielding absence or presence of open vanadium edge sites plausibly different from those in the bulk of the wall, should not affect appreciably the bulk magnetic properties.

Here, static magnetization measurements have been performed in the temperature range 2-500 K with a SQUID magnetometer from Quantum Design in magnetic fields up to 5 T and with a home-made vibrating sample magnetometer (VSM) in fields up to 15 T. Upon heating, however, we observed indication that, above ~ 370 K, the material degenerates so that we restrict the data presented here to temperatures below 370 K. Presumably this sample degradation is due to the changes of the oxygen stoichiometry. We note, however, that on the time scale of two months repeated magnetization measurements of the samples kept in air yielded identical results which assures the sample stability if overheating is avoided.

The ^{51}V -NMR experiments were carried out with a Tecmag pulse solid-state NMR spectrometer in a field of 7.05 T in a temperature range 15-285 K.

B. Static magnetization

Experiment. The temperature dependence of the static susceptibility $\chi(T) = M/H$ obtained in a magnetic field of $\mu_0H = 1$ T is shown in Fig. 2. These data are similar to the findings in Ref. 9. One can distinguish between a low-temperature regime below ~ 120 K characterized by

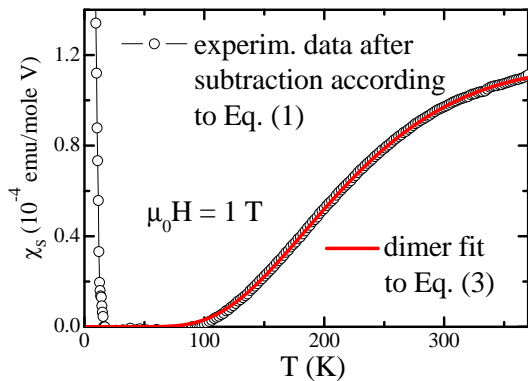


Figure 3: (Color online) High temperature contribution χ_s to the total susceptibility, Eq. (1). A fit to a dimer model, Eq. (3), is shown by a solid line (red color online) which is practically undistinguishable from the data. (For details see the text)

a Curie-like behavior, which is reflected by a linear temperature dependence of $1/\chi(T)$ (cf. Fig. 2). At higher temperatures, however, there are strong deviations from the linear behavior. The latter can be attributed to an additional contribution to the static susceptibility χ_s arising at higher temperatures. In this case χ_s can be obtained by subtracting from the raw data the Curie-Weiss term χ_{CW} and a small temperature independent contribution χ_0 owing to the Van-Vleck paramagnetism of the V ions:

$$\chi_s = \chi(T) - \chi_{CW} - \chi_0, \quad (1)$$

$$\chi_{CW} = C/(T + \Theta). \quad (2)$$

Here, $C = N_{CW} N_A \mu_B^2 / k_B$ is the Curie constant, assuming the spin $S = 1/2$ and the g factor $g = 2$, and Θ is the Curie-Weiss temperature. The best fit of the low-temperature data yields the concentration of V^{4+} spins contributing to the Curie-Weiss susceptibility $N_{CW} = 17\%$ of all V ions, $\Theta = 4$ K and $\chi_0 = 7 \cdot 10^{-5}$ emu/mole. The additional contribution χ_s is shown in Fig. 3.

Consistently with the results of Ref. 9, χ_s can be explained with a model of noninteracting antiferromagnetic dimers:

$$\chi_{dimer} = (N_d N_A \mu_B^2 / k_B) / (T[3 + \exp(\Delta/k_B T)]). \quad (3)$$

Fitting of the data in Fig. 3 to Eq. (3) implies that at $N_d = 28\%$ of all V sites there are spins $S = 1/2$ which form antiferromagnetic dimers. The dimer gap amounts to $\Delta = 710$ K. With these parameters the fit yields $\chi_s = \chi_{dimer}$ with a good accuracy.

Hence, the susceptibility data suggest that in a large temperature range the static magnetic response of VO_x -NTs can be very well described by a Curie-Weiss contribution χ_{CW} , the Van-Vleck paramagnetism χ_0 and the presence of antiferromagnetic dimers. However, below ~ 15 K the experimental data deviate from this description, (Fig. 3). Here, χ_{dimer} is practically zero owing to

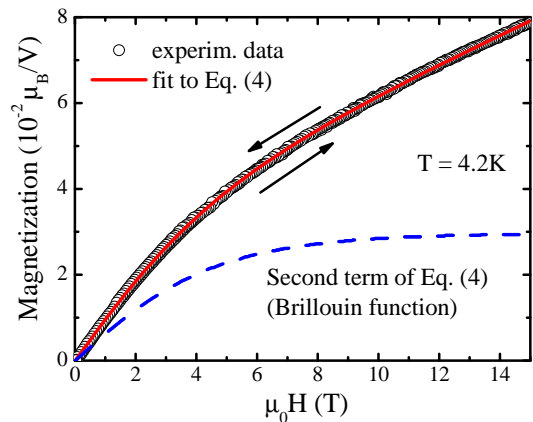


Figure 4: (Color online) Magnetic field dependence of magnetization at $T = 4.2$ K measured in ascending and descending fields. Note the absence of hysteresis. A fit to Eq. (4) is shown by a solid line (red color online) which is practically undistinguishable from the data. Contribution owing to quasi-free spins described by the Brillouin function is shown by a dashed line. (For details see the text)

a large value of Δ . Thus the strong upturn of χ_s below 15 K implies the occurrence of another contribution to the static susceptibility not accounted for in Eqs. (1) and (3). In order to address the low temperature magnetism, the field dependence of the magnetization $M(H)$ up to 15 T, at $T = 4.2$ K, has been measured. The data presented in Fig. 4 display a nearly linear field dependence of M at high magnetic fields and a pronounced curvature at lower fields without measurable hysteresis. This $M(H)$ curve can be very well fitted (Fig. 4) as a sum of two contributions

$$M(H) = \chi_{lin} H + N_B N_A \mu_B B_s(x). \quad (4)$$

The first part of Eq. (4) describes an appreciable linear contribution to M determined by a field-independent susceptibility $\chi_{lin} = 1.8 \cdot 10^{-3}$ emu/mole. The second part accounts for a nonlinearity of $M(H)$ due to the alignment of the spins by a magnetic field at low temperatures. Here $B_s(x)$ is the Brillouin function with $x = H + \lambda M$, and λ being the mean-field parameter. Assuming the g factor $g = 2$ and the spin $S = 1/2$ one obtains from the fit a small mean-field parameter $\lambda = 70$ mole/emu and the concentration of such polarisable, i.e. quasi-free, spins $N_B = 3\%$ of all V sites at $T = 4.2$ K.

Discussion. We will start the discussion of the magnetization data by considering the response at $T > 15$ K, where the susceptibility can be described well in terms of non-interacting dimers and the Curie-Weiss law. Different contributions to the magnetic susceptibility can be related to the occurrence of nonequivalent vanadium sites in the crystal structure of VO_x -NTs.⁹ The octahedrally coordinated V(1) and V(2) sites are found in the double layers (Fig. 1). Tetrahedrally coordinated V(3) sites occur between the layers. The bond valence sums calculated for a closely related material $BaV_7O_{16} \times n H_2O$

suggest that vanadium in the V(3) position has a valency close to $4+$ (d^1 , $S = 1/2$), whereas vanadium in the positions V(1) and V(2) may be $4+$ as well as $5+$ (d^0 , $S = 0$).^{7,8} The mixed-valency in $\text{VO}_x\text{-NTs}$ is confirmed by recent EELS measurements which yield 60% of V^{4+} and 40% of V^{5+} in our samples.¹⁰ Thus the concentration of magnetic V sites with $S = 1/2$ amounts to 60%. This estimate is consistent with our NMR data (see Section II C below) but, however, at first glance numerically contradicts the static magnetization data. Indeed, the number of magnetically active sites contributing to the Curie-Weiss susceptibility and to the dimer susceptibility makes up $N_{CW} + N_d = 17\% + 28\% = 45\%$ only. The number N_{CW} , however, does not necessarily count only single $S = 1/2$ V sites, which we will discuss in the following.

It is reasonable to assume that owing to magnetic frustration the V(3) spins between the layers are interacting very weakly and that all magnetic V(3) sites are therefore contributing to the Curie-like behavior of the static susceptibility.⁹ The amount of V(3) sites in the unit cell is $1/7 \approx 14\%$. A larger number of weakly interacting Curie-like $1/2$ -spins $N_{CW} = 17\%$ estimated from the analysis of the susceptibility (Fig. 2) suggests that quasi-free spins are not confined to the interlayer V(3) sites only. The mixed valency of vanadium in $\text{VO}_x\text{-NTs}$ results in a heterogeneous charge distribution in the zigzag chains comprising the walls (Fig. 1). Assuming that most of tetrahedral V(3) sites are magnetic ($\lesssim 14\%$) and recalling that the EELS data yield 40% of nonmagnetic V^{5+} ions in the structure which thus should mostly reside in the chains, one finds almost equal number of spin- ($S = 1/2$) and spinless ($S = 0$) sites in the chains. Thus, about a half of the sites in the chain are magnetic. Recalling our estimate of the concentration of spins in dimers $N_d = 28\%$ which all should reside in the chains, we obtain that those spins constitute there almost $2/3$ of magnetic chain sites. Hence, there is still a significant number of spins in the chains amounting to $\sim 18\%$ of all V sites in the unit cell, which are not coupled in dimers. If they were individual quasi-free spins, they would be expected to contribute to the Curie-Weiss susceptibility, similar to the V(3) interlayer sites. This would yield the total concentration of Curie-like spins $18\% + 14\% = 32\%$, which is almost twice as large as the experimentally determined value $N_{CW} = 17\%$. Therefore, this apparent discrepancy suggests that the remaining spins in the chain which are not involved in antiferromagnetic dimers are not independent but might form longer spin-chain fragments. Indeed, it has been recently shown both theoretically and experimentally that the ground state configuration of a strongly hole-doped antiferromagnetic Heisenberg chain is composed of spin chain fragments of different length, i.e. of spin dimers, trimers and monomers (individual spins) etc.^{11,12} Remarkably, for small external fields, trimers respond similarly to free spins at low temperatures (see e.g. Ref. 13). Thus $N_{CW} = 17\%$ of Curie-like spins estimated from

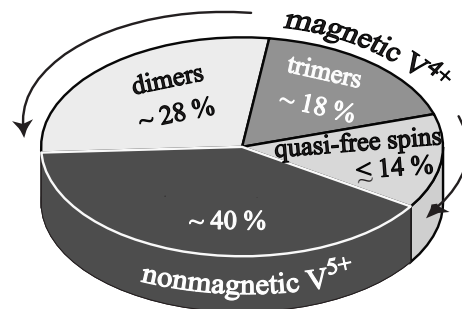


Figure 5: (Color online) Fractional weight of different spin species in $\text{VO}_x\text{-NTs}$. (For details see the text)

our susceptibility data may comprise magnetic interlayer V(3) sites, i.e. quasi-free spins, as well as trimers in the V chain.

In case of antiferromagnetic trimers, the number of magnetically active spins involved in the Curie-like response is three times larger than for single spins, i.e. for a number of spins N_t arranged in trimers only $N_t/3$ will be counted in N_{CW} . Assuming that the remaining spins in the chains which are not involved in dimers, all form trimers, i.e. $N_t = 18\%$, one obtains a correct estimate of the total concentration of magnetic $S = 1/2$ sites in the sample $(N_{CW} - N_t/3) + N_t + N_d = 57\%$, which is in a good agreement with the EELS data. To summarize the above discussion the approximate fractional weights of different spin species are depicted in the diagram in Fig. 5.

The above data analysis hence strongly suggests the occurrence in the V chains of spin-chain fragments of different lengths, i.e. individual spins, antiferromagnetic dimers and trimers. One might speculate if even longer fragments occur. The presence of chain fragments with an even number of sites, e.g. of quadrimers, however, can be ruled out by the experimental data: For quadrimers, one would expect the gap $\Delta_q = 0.659 \cdot \Delta \approx 470\text{K}$,¹³ which is not observed in our data. We also note, that the singlet-triplet excitation in the trimer occurs at $\Delta_t = 1.5 \cdot \Delta$ which can not be investigated since the sample thermally degenerates at 370 K.

Finally, we discuss the magnetization data at a low temperature $T = 4.2\text{K}$ (Fig. 4) which reveals a substantially different magnetic response as compared to the results at $T > 15\text{K}$. In particular, the concentration of quasi-free spins, i.e. monomers (individual spins) or trimers, is strongly reduced down to 3%. This clearly indicates that most of the monomers/trimers are coupled antiferromagnetically at this temperature. This scenario is corroborated by the observation of a significant linear contribution $\chi_{lin}H$ to the M vs. H curve. The fact that χ_{lin} is constant in the whole field range implies that the antiferromagnetic coupling of the monomers/trimers is larger than the energy $\mu_B H$ of the applied field of 15 T. This scenario of antiferromagnetic coupling, however, does not straightforwardly explain the *additional*

contribution to $\chi(T)$ below ~ 15 K (cf. Fig. 3). One may speculate that anisotropic coupling mechanisms, like e.g. the Dzyaloshinskii-Moriya exchange, have to be considered. This requires, however, a detailed symmetry analysis of the exchange paths between vanadium spins in VO_x -NTs.

C. Nuclear Magnetic Resonance

Experiment. The ^{51}V -NMR experiments were carried out in a field of 7.05 T in a temperature range 15-285 K. ^{51}V nucleus has a spin $I = 7/2$ and possesses a nuclear quadrupole moment. Therefore it is sensitive to both, the magnetic degrees of freedom and to the charge environment. The NMR spectra were acquired by a point-by-point frequency sweeping. At each frequency point the signal has been obtained by a Fourier transformation of the Hahn spin echo $\pi/2 - \tau - \pi$ with the pulse separation time $\tau = 13 \mu\text{s}$. The final frequency-swept spectrum has been calculated by sequential summing of the signals at three successive frequency points. In Fig. 6 a spectrum at $T = 285$ K is shown as an example. The spectrum is broadened due to a different orientation of nanotubes in a powder sample and contains several unresolved quadrupole satellites. The relaxation times T_2 and T_1 were measured at the frequency of the maximum intensity of the spectrum which was assigned to the main $|+1/2\rangle \leftrightarrow |-1/2\rangle$ NMR transition. The transversal relaxation time T_2 has been determined from the Hahn spin echo decay which cannot be described by a single exponent. However it could be very well fitted assuming the two-exponential behavior with two distinctly different relaxation times. To measure the longitudinal relaxation time T_1 a method of stimulated echo employing a pulse sequence $\pi/2 - t - \pi/2 - \tau - \pi/2$ with $t < \tau$ has been used. The time dependence of the stimulated spin echo intensity $A_{st}(\tau)$, which is a measure of the decay of the longitudinal magnetization characterized by the relaxation time T_1 , has been analyzed following the standard equation for the spin $I = 7/2$ derived in Ref. 14. Also in this case the decay of $A_{st}(\tau)$ cannot be described by a one-center fitting. The fit requires the presence of two contributions of different weights with distinctly different relaxation rates. Thus for the following discussion it is useful to define the "fast" and the "slow" relaxation processes. The temperature dependence of the "fast" and "slow" transverse and longitudinal relaxation rates T_2^{-1} and T_1^{-1} is shown in Fig. 7. The "slow" contribution to T_2^{-1} is temperature independent whereas the "fast" one as well as both contributions to T_1^{-1} increase with increasing temperature. The ratio of the weights of these two contributions to the relaxation decay $k_{fast} : k_{slow}$ at $T = 285$ K is close to 2.4. However the weight of the "slow" component strongly increases with decreasing temperature yielding $k_{fast} : k_{slow} \approx 0.7$ at $T = 15$ K (Fig. 8).

Discussion. As discussed in Section II B vanadium ions

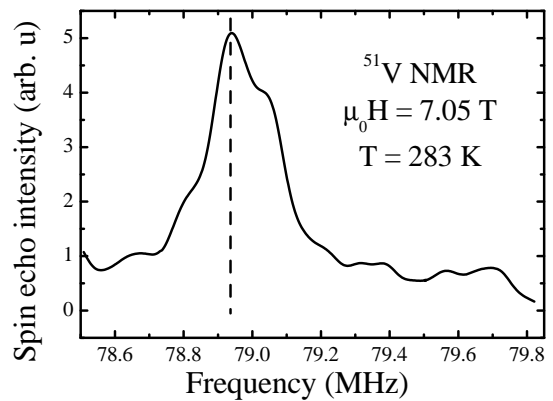


Figure 6: ^{51}V -NMR spectrum of a VO_x -NT sample at $T = 285$ K. The dashed line indicate the frequency of the maximum intensity at which the relaxation measurements have been carried out.

in VO_x -NTs occur in different valence states and can be magnetic and nonmagnetic. The ions possessing an electronic magnetic moment produce a fluctuating magnetic field at the nuclei. It leads to a fast relaxation of the nuclei of the magnetic ions due to the on-site hyperfine interaction. The magnitude of the transferred hyperfine field at the nuclei of nonmagnetic ions is much smaller and the relaxation is more slow. The temperature independent "slow" component of T_2^{-1} can obviously be assigned to the conventional magnetic dipolar interaction (see, e.g., Ref. 15). However with increasing temperature a more effective relaxation channel appears. The fact that the temperature dependence of the "fast" T_2^{-1} contribution is similar to that of the both components of T_1^{-1} (Fig. 7) gives evidence that the origin of this contribution is the relaxation due to the fluctuating magnetic field produced by electron spins at the nuclei. In this case according to the Redfield's theory¹⁶ T_1^{-1} and T_2^{-1} are determined by the magnitude of the transferred field H_i ($i = x, y,$ and z) and the correlation time τ_0 of the electron spins:

$$T_1^{-1} = \gamma_n^2 [\overline{H_x^2} + \overline{H_y^2}] \tau_0 / (1 + \omega_n^2 \tau_0^2), \quad (5)$$

$$T_2^{-1} = \gamma_n^2 [\overline{H_z^2} \tau_0 + \overline{H_y^2} \tau_0 / (1 + \omega_n^2 \tau_0^2)]. \quad (6)$$

Here γ_n is the nuclear gyromagnetic ratio and ω_n is the NMR frequency, respectively. In the regime of fast fluctuations, $\omega_n \tau < 1$, which is expected far away from magnetically ordered phases, the observed strong increase of the relaxation rates with temperature (Fig. 7a) suggests the enhancement of H_i at the positions of the nuclei owing to, e.g., an increase of the concentration of the spin centers. Moreover, the change of the ratio of the weight coefficients of two contributions to the relaxation decay $k_{fast} : k_{slow}$ with temperature (Fig. 8) can be explained by taking into account the magnetic susceptibility data which indicate that part of magnetic ions form antiferromagnetic dimers and exhibit a spin gap behavior. Usually owing to a spin gap the huge slowing down of relaxation with decreasing temperature is observed, as, e.g. in

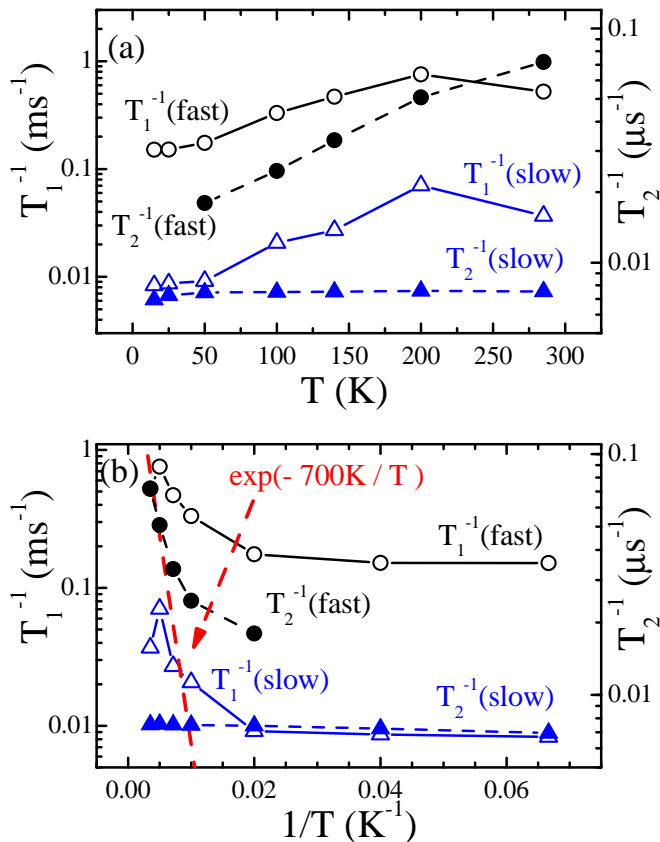


Figure 7: (Color online) "Fast" and "slow" contributions to the NMR relaxation rates T_1^{-1} and T_2^{-1} : (a) as a function of temperature; (b) as a function of inverse temperature. Dashed line denotes the expected behavior of T_1^{-1} according to Eq. (7) due to the opening of the spin gap $\Delta \sim 700$ K.

the case of the low-dimensional vanadium oxides, it has been observed in the NMR relaxation measurements of a two-leg spin-ladder CaV_2O_5 ,^{17,18} or a quarter-filled ladder compound NaV_2O_5 .¹⁹ The occurrence of a spin gap Δ yields an exponential temperature dependence of the longitudinal relaxation rate T_1^{-1} for $T < \Delta$.^{20,21}

$$T_1^{-1} \propto \exp(-\Delta/T)[0.80908 - \ln(\omega_n/T)]. \quad (7)$$

With the dimer gap $\Delta = 710$ K deduced from our magnetization data one would expect a strong decrease of the nuclear relaxation below 100 K, which is not observed experimentally (cf. Fig. 7). Obviously, in our case this picture is disguised by the presence of nondimerized magnetic ions providing fast relaxation even at low temperature. These magnetic centers can be assigned to the interlayer V(3) sites as well as to trimers in the V chains (see Section II B). The nuclei in dimerized ions are slowly relaxing at low temperatures because of the non-magnetic singlet ground state of a dimer and fast relaxing at high temperatures owing to thermally activated singlet-triplet excitations across the dimer gap. Hence the existence of a spin gap should be seen as a change of the weight coefficients of the respective T_1^{-1} contri-

butions. Moreover, thermal activation of dimers at high temperatures should effectively look like an increase of the concentration of magnetic centers. This should enhance the magnitude of the fluctuating magnetic field and the relaxation rate of the "slow-relaxing" nuclei. Indeed, as can be seen in Fig. 8 with increasing temperature the relaxation rate of the "slow" nuclei grows stronger than that of the "fast" ones. The common temperature dependence of the ratios of the weights and of the relaxation times of two contributions (Fig. 8) justifies the same origin of both dependences which can be due to the occurrence of the spin gap for a part of magnetic vanadium ions. The weight coefficients at high temperatures provides the ratio of the fast and slow relaxing centers approximately as 70%:30%. This ratio is in a fair agreement with the EELS estimation of the ratio between magnetic V^{4+} and nonmagnetic V^{5+} amounting to 60%:40%.¹⁰ Therefore in the high temperature regime it is reasonable to associate the fast- and the slow-relaxing centers with V^{4+} and V^{5+} sites, respectively. From the weight ratio $k_{fast} : k_{slow}$ at low temperatures one obtains the number of "slow-relaxing" nuclei amounting to $\approx 60\%$ which comprises the nonmagnetic V^{5+} sites as well as the dimerized centers. As the high-temperature NMR estimate of the V^{5+} sites amounts to $\approx 30\%$, the concentration of the magnetic $S = 1/2$ V^{4+} sites coupled in antiferromagnetic dimers is, therefore, about 30% of all vanadium, in a good agreement with the estimate $N_d = 28\%$ from the static magnetization data (Section II B). The NMR estimate of the "fast-relaxing", i.e. paramagnetic centers, at low temperatures yields $\approx 40\%$ which is significantly larger than the concentration of the Curie-like spins $N_{cw} = 17\%$ obtained from the analysis of the Curie-like susceptibility χ_{cw} (Eq. 2). This apparent contradiction can be resolved if not only individual spins but also trimers would contribute to χ_{cw} at low temperatures, as has been suggested in the analysis of the static magnetic data in Section II B. Assuming that the nuclei in a trimer belong to the "fast-relaxing" centers, owing to a magnetic ground state of a trimer, all N_t sites involved in trimers will be counted in the weight of the respective contribution to the NMR relaxation rate T_1^{-1} , whereas effectively only $N_t/3$ of those sites is counted in N_{cw} . Thus the analysis of the NMR data strongly supports the static magnetic results, both justifying the occurrence of comparable amounts of individual spins, antiferromagnetic dimers and trimers as depicted in Fig. 5.

III. CONCLUSIONS

In summary, magnetization and ^{51}V NMR measurements of the samples of multiwalled vanadium-oxide nanotubes reveal a complex evolution of the static and dynamic magnetic properties as a function of temperature. The results give strong indications that different spin arrangements beyond a simplified picture suggested

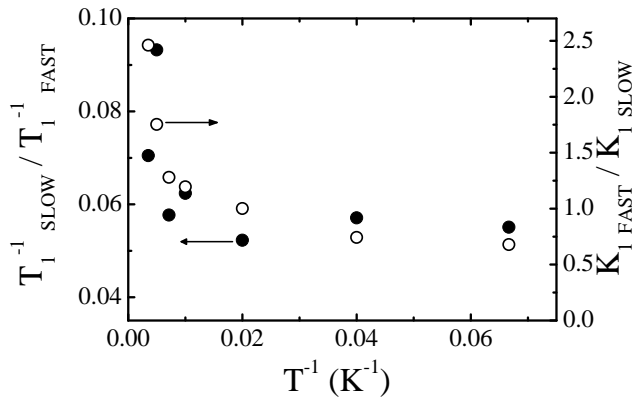


Figure 8: Dependence on the inverse temperature of the ratio of the "slow" and "fast" contributions to the NMR relaxation rate T_1^{-1} on the ratio of the weights of these contributions $k_{fast} : k_{slow}$.

in Ref. 9 are realized in VO_x -NTs. In particular, the data analysis strongly suggests that in addition to individual spins and antiferromagnetic dimers showing a spin gap of the order of 700 K an appreciable amount of spin

trimers occur in the samples. Though the estimate of the fractional weights of different spin species summarized in Fig. 5 might change to some extent owing to the experimental uncertainties, and also because structural imperfections as well as the proportion of the majority scrolled tubes to the minority concentric tubes may vary to some extent from sample to sample, the data give evidence for the coexistence of different spin configurations in comparable amounts which is related to the complex low-dimensional crystallographic structure as well as mixed valency of this nanoscale magnet.

IV. ACKNOWLEDGMENTS

This work was supported by the Deutsche Forschungsgemeinschaft (DFG) through project KL 1824/2. The work of EV was supported by the DFG grant 436RUS17/38/06, joint DFG - Russian Academy of Sciences project on physics of novel materials 436RUS113/780/0-1 and also by the Russian Foundation for Basic Research through grant No. 04-02-17137.

-
- ¹ F. J. Himpsel, J. E. Ortega, G. J. Mankey, and R. F. Willis, *Adv. Phys.* **47** 511 (1998).
 - ² M. Imada, A. Fujimori, and Y. Tokura, *Rev. Mod. Phys.* **70**, 1039 (1998).
 - ³ E. Dagotto, *Rep. Prog. Phys.* **62**, 1525 (1999).
 - ⁴ J. Tokura and Y. Nagaosa, *Science* **288**, 462 (2000).
 - ⁵ J. Orenstein and A. J. Millis, *Science* **288**, 468 (2000).
 - ⁶ F. Krumeich, H.-J. Muhr, M. Niederberger, F. Bieri, B. Schnyder, and R. Nesper, *J. Am. Chem. Soc.* **121**, 8324 (1999).
 - ⁷ M. Wörle, F. Krumeich, F. Bieri, H.-J. Muhr, and R. Nesper, *Z. Anorg. Allg. Chem.* **628**, 2778 (2002).
 - ⁸ X. Wang, L. Liu, R. Bontschev, and A. J. Jacobson, *J. Chem. Soc. Chem. Commun.* 1009 (1998).
 - ⁹ L. Krusin-Elbaum, M. N. Newns, H. Zeng, V. Dericke, J. Z. Sun, and R. Sandstrom, *Nature* **431**, 672 (2004).
 - ¹⁰ X. Liu, C. Täschner, A. Leonhardt, M.-H. Rummeli, T. Pichler, T. Gemming, B. Büchner, and M. Knupfer, *Phys. Rev. B* **72** 115407 (2005).
 - ¹¹ A. Gelle and M. B. Lepetit, *Phys. Rev. Lett.* **92** 236402 (2004).
 - ¹² R. Klingeler, B. Büchner, K.-Y. Choi, V. Kataev, U. Ammerahl, A. Revcolevschi, and J. Schnack, *Phys. Rev. B* **73**, 014426 (2006).
 - ¹³ R. Klingeler, N. Tristan, B. Büchner, M. Hücker, U. Ammerahl, and A. Revcolevschi, *Phys. Rev. B* **72**, 184406 (2005).
 - ¹⁴ A. Narath, *Phys. Rev.* **162**, 320 (1967).
 - ¹⁵ J. Ph. Ansermet, C. P. Slichter, and J. H. Sinflet, *J. Chem. Phys.* **88**, 5963 (1988).
 - ¹⁶ C. P. Slichter, *Principles of Magnetic Resonance*, 3rd ed., (Springer, New York, 1989).
 - ¹⁷ H. Iwase, M. Isobe, Y. Ueda, H. Yasuoka, *J. Phys. Soc. Jpn.* **65**, 2397 (1996).
 - ¹⁸ T. Ohama, M. Isobe, and Y. Ueda, *J. Phys. Soc. Jpn.* **70**, 1801 (1996).
 - ¹⁹ T. Ohama, H. Yasuoka, M. Isobe, and Y. Ueda, *Phys. Rev. B* **59** 3299 (1999).
 - ²⁰ M. Troyer, H. Tsunetsugu, and D. Würtz, *Phys. Rev. B* **50** 13515 (1994).
 - ²¹ F. Naef and X. Wang, *Phys. Rev. Lett.* **84**, 1320 (2000).